

Performance Assessment of Rubberized Mixtures Containing Reclaimed Asphalt and a Viscosity Reduction Additive

Original

Performance Assessment of Rubberized Mixtures Containing Reclaimed Asphalt and a Viscosity Reduction Additive / Urbano, Leonardo; Dalmazzo, Davide; Riviera, Pier Paolo; Santagata, Ezio (LECTURE NOTES IN CIVIL ENGINEERING). - In: Proceedings of the 9th International Conference on Maintenance and Rehabilitation of Pavements—Mairepav9 / Christiane Raab. - ELETTRONICO. - [s.l.] : Springer Nature, 2020. - ISBN 978-3-030-48678-5. - pp. 457-467 [10.1007/978-3-030-48679-2_43]

Availability:

This version is available at: 11583/2837074 since: 2020-07-08T09:34:57Z

Publisher:

Springer Nature

Published

DOI:10.1007/978-3-030-48679-2_43

Terms of use:

This article is made available under terms and conditions as specified in the corresponding bibliographic description in the repository

Publisher copyright

Springer postprint/Author's Accepted Manuscript

This version of the article has been accepted for publication, after peer review (when applicable) and is subject to Springer Nature's AM terms of use, but is not the Version of Record and does not reflect post-acceptance improvements, or any corrections. The Version of Record is available online at: http://dx.doi.org/10.1007/978-3-030-48679-2_43

(Article begins on next page)

Performance assessment of rubberized mixtures containing reclaimed asphalt and a viscosity reduction additive

Leonardo Urbano, Davide Dalmazzo, Pier Paolo Riviera, Ezio Santagata *

Department of Environment, Land and Infrastructure Engineering, Politecnico di Torino
24, Corso Duca degli Abruzzi, 10129 Italy
ezio.santagata@polito.it

Abstract This paper illustrates the results obtained in a study which focused on the mix design and performance-related characterization of rubberized dense-graded mixtures containing a viscosity reduction additive and different percentages of reclaimed asphalt. Following preliminary mix design, plant-produced mixtures were employed for the construction of full-scale trial sections and were subjected to standard quality assurance tests and to advanced mechanical characterization tests. Analysis of results was performed by referring to typical acceptance thresholds and to the outcomes of simplified viscoelastic continuum damage modelling. It was concluded that reclaimed asphalt can have a non-negligible effect on performance properties and that the considered rubberized mixtures, which can be compacted at reduced temperatures, are suitable for paving applications.

Keywords: rubberized asphalt mixture, reclaimed asphalt, viscosity reduction additive, dynamic modulus, flow number, fatigue, viscoelastic continuum damage.

1 Introduction

Recycling of waste materials and preservation of the ecosystem and of natural resources are fundamental needs which have to be taken into account in the design of today's civil infrastructures. In such a context, new asphalt pavements are designed in a framework in which sustainability is a key concept. In the specific case of bituminous mixtures employed in paving applications, the combined use of crumb rubber (CR) derived from end-of-life tires as a modifier of asphalt binders and of reclaimed asphalt (RA) as a partial substitute of virgin aggregates is a technology that can lead to significant benefits in terms of energy saving, environmental impact, human health, and preservation of ecosystems (Farina et al., 2017; Pouranian and Shishehbor, 2019). Furthermore, rubberized asphalt mixtures containing RA have shown improved mechanical properties and performance in terms of indirect tensile strength, moisture susceptibility, resilient modulus and rutting resistance (Xiao et al., 2007; Xiao et al., 2008). In these mixtures the viscosity of the binder is greatly increased by the presence of CR particles (Xiao et al., 2008; Santagata et al., 2012), thus leading to a significant

increase of mixing and compaction temperatures. The use of viscosity reduction additives, conventionally used for warm mix asphalt, can help to reduce these temperatures thereby leading to a reduction of emissions and to a lower energy consumption in mix production and compaction. The adoption of such a solution is encouraged by the fact that several experimental works (Behroozikhah et al. 2017; Mogawer et al., 2013; Saberi et al., 2017) have shown that rubberized mixtures containing RA and viscosity reduction additives exhibit an improved performance in terms of stiffness, rutting resistance and fatigue life.

The Authors of this paper have addressed a multitude of issues related to the use of rubberized mixtures in road pavements as part of the “TYREC4LIFE” project funded by the European Commission through its “LIFE+” program. Investigations were carried out in the laboratory and in the field, with the evaluation of several alternative solutions that entailed the production of gap-graded and dense-graded mixtures by means of dry and wet technologies (Zanetti et al., 2014, 2015; Santagata et al., 2015, 2016). Due to the encouraging results obtained during its development, the project was followed by supplementary activities, funded by the Italian Ministry of the Environment, Land and Sea, which were focused on the evaluation of rubberized mixtures of premium sustainability containing RA and viscosity reduction additives. This paper provides a synthesis of some of the activities which were undertaken in the “TYREC4LIFE” follow-up project.

2 Experimental program

The investigation illustrated in this paper focused on dense-graded wearing course rubberized mixtures containing RA and viscosity reduction additives. The experimental program included an initial mix design phase (including characterization of component materials) and a further phase of assessment of plant-produced mixtures which were laid in full-scale field trial sections.

Mix design activities considered three different dense-graded mixtures – indicated as ARS0, ARS10 and ARS20 – containing increasing quantities of RA (with dosages by weight of total aggregates equal to 0%, 10% and 20%, respectively). Mixture AS0, with no RA, was included in the study for comparative purposes.

Following their mix design, the mixtures containing RA were manufactured in a batch plant (with corresponding codes ARS10-P and ARS20-P) and laid on site for the construction of a pavement wearing course of an urban road. During construction, loose mixtures were sampled with the purpose of performing standard quality assurance (QA) tests and advanced mechanical characterization tests. The QA assessment included tests for the evaluation of the volumetrics of Marshall and gyratory-compacted specimens, Marshall stability and indirect tensile strength. Advanced mechanical characterization included tests for the evaluation of the dynamic modulus master curve, flow number and fatigue life.

3 Materials and methods

The rubberized binder considered in the study was an asphalt rubber (AR), provided by an Italian supplier, fabricated by mixing a 50/70 penetration grade bitumen with 20% CR. Particles constituting CR were entirely passing the 1.18 mm sieve in accordance to ASTM D6114.

The viscosity reduction additive employed to decrease mixing and compaction temperatures of bituminous mixtures was a synthetic microcrystalline wax produced by means of coal gasification, characterized by the presence of long chain aliphatic hydrocarbons (Jamshidi et al., 2013). Based on manufacturer's recommendations, a dosage of 3% by weight of binder was adopted during the entire investigation. In the laboratory, the additive was blended with the AR binder at 190 °C by means of a mechanical mixer operating at a constant speed of 400 rpm for 10 minutes.

The original AR and the AR containing the additive (ARS) were preliminarily characterized in terms of their penetration at 25 °C (EN 1426) and of their softening point (EN 1427). Furthermore, they were subjected to frequency sweep tests (EN 14770) for the construction of the master curves of the norm and phase angle of the complex modulus at a reference temperature of 34 °C. Tests were carried out with a dynamic shear rheometer equipped with parallel plates of variable diameter (25 mm or 8 mm), operated in the frequency range of 1-100 rad/s and in the temperature range of 0-82 °C. Dynamic viscosity tests (EN 13302) were carried out by making use of a rotational viscometer equipped with a cylindrical spindle rotating at constant shear rate of 6.8 s⁻¹ in the temperature range comprised between 125 °C and 175 °C.

Bituminous mixtures were prepared by employing three locally-available aggregate fractions (10/15 mm, 3/8 mm and 0/8 mm), a mineral filler and RA material obtained from the milling of wearing courses. Particle size distribution analyses of aggregates and RA, before and after binder extraction, were carried out according to EN 933-1. RA binder content was determined as per EN 12697-39. For the three mixtures considered in design (ARS0, ARS10 and ARS20), fractions were combined in order to yield the same target gradation, typical of dense-graded wearing courses.

Optimum binder content of each mixture was identified by considering different binder contents for each combination of aggregate fractions, filler and RAP. For each binder content, four Marshall specimens (EN 12697-30, 75 blows per side) and four gyratory specimens (EN 12697-31, 100 gyrations) were compacted at 155 °C. Volumetric properties (EN 12697-5, -6, -8) were assessed for both sets of specimens. Thereafter, Marshall tests (EN 12697-34) and indirect tensile strength (ITS) tests at 25 °C (EN 12697-23) were performed on Marshall specimens and gyratory specimens, respectively. Optimum binder content was identified based on acceptance criteria defined in terms of Marshall air voids content (3-6%), Marshall stability (≥ 9 kN) and Marshall flow (≥ 2 mm). ITS results were considered as supplementary information which supported the choice derived from simple Marshall design.

QA tests and advanced mechanical tests were carried out on the ARS10-P and ARS20-P mixtures manufactured in the asphalt plant and sampled during paving operations. In addition to the specimens required for the QA assessment, six specimens

180 mm thick and 150 mm in diameter were compacted at 155 °C with 40 gyrations of the gyratory compactor for each mixture. The specimens were then cored and trimmed to obtain testing samples 150 mm thick and 100 mm in diameter (AASHTO PP 60). The number of gyrations equal to 40 was defined by means of a preliminary volumetric analysis which showed that they were those necessary in order to obtain a target air voids content of $8.0\% \pm 0.5\%$.

Cyclic uniaxial compression tests (AASHTO T 378) at three temperatures (4 °C, 20 °C and 40 °C) and six frequencies (25 Hz, 10 Hz, 5 Hz, 1 Hz, 0.5 Hz and 1 Hz) were performed on all ARS10-P and ARS20-P specimens by applying an axial strain of approximately $100 \cdot 10^{-6}$ mm/mm, with the consequent evaluation of dynamic modulus and phase angle. Flow number (FN) was obtained as the average of three replicates from repeated load permanent deformation tests (AASHTO T 378) carried out at 58 °C by applying load pulses of 600 kPa with a 0.1 s duration every 1 s. Resistance to fatigue cracking was investigated by means of time sweep tests (AASHTO TP 107) performed at three strain levels, in the direct tension configuration and in the strain-controlled mode, at 18 °C and 10 Hz. The first peak-to-peak strain was set equal to $300 \cdot 10^{-6}$ mm/mm, while the second and the third strain levels were selected as function of the failure cycles obtained during the first test.

4 Results and discussion

4.1 Characterization of component materials and mix design

The original AR was characterized by a penetration of 29 dmm and a softening point of 73 °C. Addition to the AR of the viscosity reduction additive led to important changes in consistency, with the consequent reduction of penetration (25 dmm) and increase of softening point (101 °C).

These results were consistent with those obtained from frequency sweep tests, which are displayed in Fig. 1a in the form of master curves of the norm of the complex modulus and of the phase angle (at 34 °C). It can be observed that binder ARS exhibited complex modulus values which were higher than those of binder AR at low and intermediate frequencies, while similar values were recorded at high frequencies. On the contrary, the phase angle was slightly reduced by the presence of the viscosity reduction additive mainly at intermediate frequencies. These effects can be explained by the presence of a crystalline structure in the additive which may provide an enhanced stiffness and elasticity to the ARS binder.

As proven by the results of viscosity tests (Fig. 1b), the abovementioned stiffening effects were lost at temperatures above the melting point of the employed wax (i.e. above 115 °C), where binder ARS displayed a viscosity which was significantly lower than that of the original AR. Based on these results, compaction temperature of the rubberized mixtures was set at 155 °C, at which the viscosity of the ARS binder was in the 1.5-5 Pa·s range, often referred to in specifications for acceptance purposes.

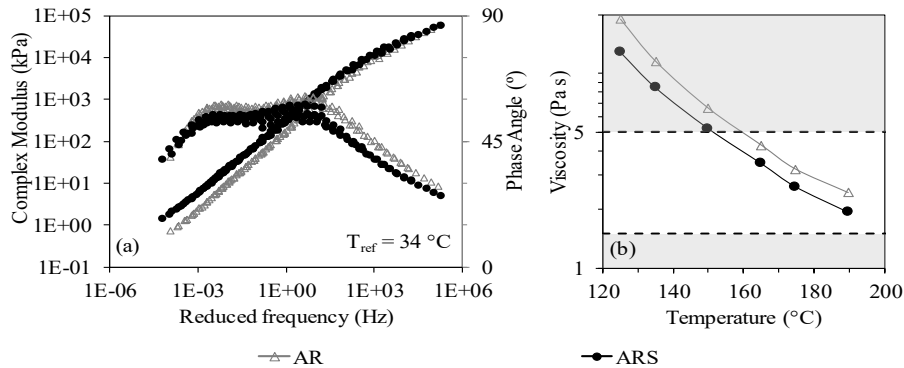


Fig. 1 Complex modulus and phase angle master curves (a) and dynamic viscosity (b) of binders AR and ARS

Table 1 RA gradation before and after binder extraction, gradation limits and job mix formula for design mixtures ARS0, ARS10 and ARS20

Sieve size (mm)	RA black curve (%)	RA white curve (%)	Gradation limits (%)	Job Mix Formula (%)
12.5	100	100	100-100	100
10	100	100	87-96	92
8	95.7	98.0	70-90	83
6.3	80.9	87.0	60-80	67
4	55.2	64.4	40-60	51
2	32.8	41.9	25-38	33
1	17.9	29.1	19-30	24
0.5	8.7	21.3	13-22	17
0.063	0.4	8.2	6-9	7.5

Based on the results obtained from particle size distribution analyses (Table 1), the RA material was classified as 10RA0/8, while its binder content coming from ignition tests was found to be equal to 6.8% by the total weight of RA.

Design of the three mixtures included in the study (ARS0, ARS10 and ARS20) was performed by referring to typical specification limits adopted for dense-graded wearing courses and by considering a single target gradation (Table 1).

Results collected in the mix design phase are shown in Fig. 2, where the average values of various volumetric and mechanical parameters are plotted, for each mixture, as a function of binder content (%B), expressed as the percentage of added ARS by the total weight of aggregates (virgin and RA). Additional data points which are shown in Fig. 2 (with indicators filled in black) refer to the results obtained in the QA of the plant-produced mixtures (discussed in section 4.2).

It can be observed that the introduction of RA into the mixtures led to a reduction of air void contents (Fig. 2a and Fig. 2b), probably as a result of the presence of the additional binder covering the RA particles which may allow these to more easily adapt to the packed configuration reached during compaction. The resulting higher

density and the presence of the aged RA binder also led to an overall increase of stiffness and strength, as shown by the higher Marshall stability (Fig. 2c) and ITS (Fig. 2d). The presence of the additional binder coming from the RA, which reflected in a TMD reduction (Fig. 2f), also provided the mixtures with a more ductile behaviour, demonstrated by the higher values of Marshall flow (Fig. 2e).

Based on the results discussed above, optimum binder contents selected for the mixtures containing RA were equal to 5.5% and 4.5% (by total weight of aggregates) for mixtures ARS10 and ARS20, respectively.

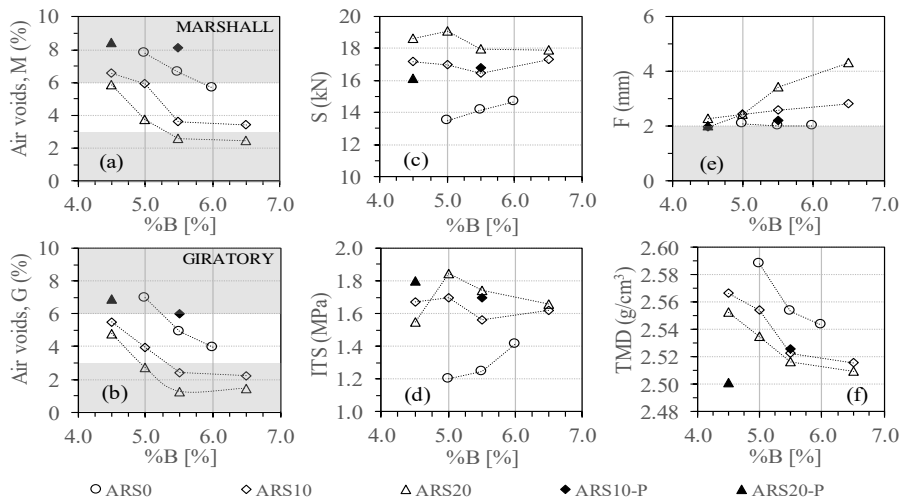


Fig. 2 Mix design and quality assurance results: Marshall air voids content (a), gyratory air voids content (b), Marshall stability, S (c), ITS (d), Marshall flow, F (e), and theoretical maximum density, TMD (f)

4.2 Quality assurance and performance-related evaluation

The two rubberized mixtures containing RA were manufactured at 175 °C in a batch asphalt plant located 15 km from the construction site. Average compaction temperatures recorded during paving, slightly lower than target, were equal to 145 °C and 153 °C for mixtures ARS10-P and ARS20-P, respectively.

Total binder content (by weight of aggregates) derived from ignition tests was equal to 5.9% and 5.8% for mixtures ARS10-P and ARS20-P, respectively. By assuming the presence of the design RA dosages, these values correspond to dosages of added binder equal to 5.25% and 4.5%, which are very close to optimal mix design values.

Aggregate gradation showed significant deviations from target for both mixtures, probably as a result of inconsistencies occurring in the filler dosage system at the plant. While such a problem mainly reflected in the low filler content of mixture ARS10-P (equal to 5.7%), it affected the entire fine fraction of mixture ARS20-P, with very low percentages passing the 1.0 mm, 0.5 mm and 0.063 mm sieves (equal to 18.6%, 12.7% and 4.5%, respectively).

As mentioned in section 4.1, the black indicators displayed in Fig. 2 refer to the volumetric and mechanical properties of the two plant-produced mixtures. Thus, it can be observed that the very high values of air voids contents of both Marshall and gyratory specimens, probably due to the lack of filler, were not consistent with design values and did not satisfy specification limits. On the contrary, Marshall stability and ITS values were similar to those coming from design.

In order to derive master curves at a reference temperature of 20 °C, complex modulus data collected at different temperatures and frequencies were fitted to the sigmoidal model (Bonaquist and Christensen, 2005) and to the Arrhenius equation given in Eq. (1) and (2), respectively. The limiting maximum modulus was estimated from the composition and volumetrics of the mixtures by making use of the relationships indicated in AASHTO T 378.

$$\log|E^*| = \delta + \frac{(\text{Max} - \delta)}{1 + e^{\beta + \gamma \log f_r}} \quad (1)$$

$$\log a(T) = \frac{\Delta E_a}{19.14714} \left(\frac{1}{T} - \frac{1}{T_r} \right) \quad (2)$$

where $|E^*|$ is the norm of the complex modulus (MPa), Max is the limiting maximum modulus, f_r is the reduced frequency (Hz), $a(T)$ is the shift factor at the generic test temperature T (K), T_r is the reference temperature (K), and δ , β , γ , ΔE_a are fitting parameters.

Master curves are represented in Fig. 3, while corresponding model parameters are listed in Table 2. It can be observed that mixture ARS-20P was characterized by a higher stiffness and greater elasticity (i.e. lower phase angle) with respect to mixture ARS-10P. These outcomes are consistent with the higher RA content and lower volume of binder which differentiates mixture ARS-20P from mixture ARS-10P.

Table 2 Master curve parameters of mixtures ARS-10P and ARS-20P

	$ E^* _{\text{Max}}$ (GPa)	δ (-)	β (-)	γ (-)	ΔE_a (kJ/mol)
ARS-10P	21.074	2.96	-1.44	-0.37	202
ARS-20P	21.145	3.03	-1.52	-0.38	211

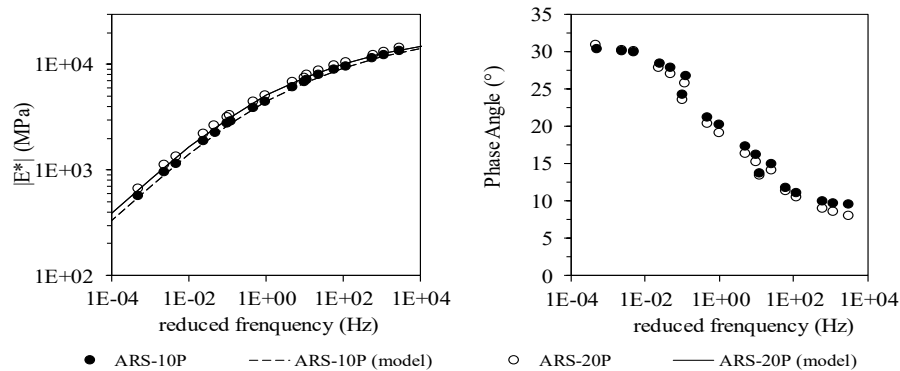


Fig. 3 Master curves of mixtures ARS-10P and ARS-20P

Experimental data recorded during repeated load permanent deformation tests were analysed by making use of the model proposed by Francken, given in Eq. (3), which is capable of describing the primary, secondary and tertiary stages of the flow process (Biligiri et al., 2007).

$$\varepsilon_p(N) = AN^B + C(e^{DN} - 1) \quad (3)$$

where ε_p is the permanent axial strain in 10^{-6} mm/mm, N is the number of loading cycles and A , B , C and D are the fitting parameters.

Average N - ε_p curves obtained for the two mixtures are displayed in Fig. 4a in which the points corresponding to the FN values, that identify the number of load repetitions at which shear deformation under constant volume is initiated, are also highlighted. This information is supplemented by the data listed in Table 3, which contains average FN values and the corresponding model fitting parameters. As in the case of linear viscoelastic characterization (Table 2 and Fig. 3), the stiffening effect caused by increasing quantities of RA in the mixtures is clearly visible. Thus, mixture ARS20-P was found to be more rut resistant than mixture ARS10-P.

Table 3 FN values and model fitting parameters of mixtures ARS-10P and ARS-20P

	FN	A	B	C	D
ARS-10P	935	2,171.0	0.36269	409.62	0.001837
ARS-20P	1,498	1,726.1	0.37306	49.84	0.002020

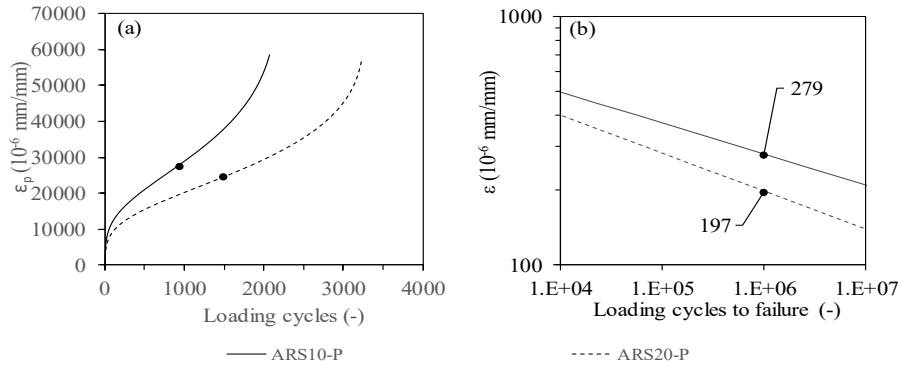


Fig. 4 Results obtained from FN tests (a) and fatigue damage modelling (b)

Results obtained in time sweep tests performed on specimens of the two plant-produced rubberized mixtures were modelled by making use of the so-called simplified viscoelastic continuum damage approach (S-VECD). In particular, by following the procedures suggested by Underwood et al. (2012), experimental data were fitted to Eq. (4) and to Eq. (5), thereby obtaining the damage characteristic curve and the number of cycles to failure corresponding to any given strain. Fatigue curves were then derived for both mixtures as shown in Fig. 4b, where the strain level corresponding to one million loadings to failure (ε_6) is explicitly highlighted.

$$C(S)=1-C_{11} S^{C_{12}} \quad (4)$$

$$N_{\text{failure}} = \frac{(f_{\text{red}})(2^{3\alpha})S_f^{\alpha-C_{12}+1}}{(\alpha-C_{12}+1)(C_{11}C_{12})^\alpha [(\beta+1)(\varepsilon_{0,\text{pp}})(|E^*|_{\text{LVE}})]^{2\alpha} K_1} \quad (5)$$

where S is damage, $C(S)$ is the pseudo-secant modulus, C_{11} and C_{12} fitting parameters, f_{red} is the reduced frequency, α is the damage evolution rate, S_f is the cumulative damage at the failure point, β is the load form factor, $\varepsilon_{0,\text{pp}}$ is the peak-to-peak strain magnitude, $|E^*|_{\text{LVE}}$ is the norm of the complex modulus and k_1 is the loading shape factor. Calculated values of all the abovementioned fitting coefficients are listed in Table 4.

Table 4 Damage model fitting parameters

	C_{11} (-)	C_{12} (-)	f_{red} (Hz)	α (-)	S_f (-)	β (-)	$ E^* _{\text{LVE}}$ (GPa)	K_1 (-)
ARS-10P	0.0056	0.4078	17.9	4.0	104627	0	7.1	0.27
ARS-20P	0.0034	0.4598	17.8	3.3	66961	0	7.6	0.30

It was observed that the stiffening effects related to the presence of increasing quantities of RA in the mixtures had a negative impact on their response under repeated loading in terms of their fatigue resistance. In particular, as clearly shown in Fig. 4b, mixture ARS-20P had a fatigue life which was shorter than that of mixture ARS-10P.

4 Conclusions

The experimental results obtained in the investigation described in this paper indicate that in the design of rubberized mixtures it is possible to successfully combine the use of reclaimed asphalt and of viscosity reduction additives. A proper use of the additives may allow compaction temperatures to be reduced by 15 °C, while the introduction of reclaimed asphalt in the bearing skeleton of the mixtures can simultaneously lead to an increase of their density and to an overall enhancement of stiffness, elasticity and resistance to rutting. Residual concerns may be related to the fatigue properties of these mixtures, for which further refinements in mix design may be necessary.

Although the considered rubberized mixtures seem to be suitable for paving applications, it is envisioned that more research is needed in order to fully exploit their performance potential and to develop comprehensive mix design guidelines and technical specifications. Furthermore, additional analyses are recommended for a full quantitative assessment of the sustainability benefits which they bring to pavement construction and maintenance.

References

- Behroozikhah, A., Morafa, S.H., Aflaki, S., 2017. Investigation of fatigue cracks on RAP mixtures containing Sasobit and crumb rubber based on fracture energy. *Constr. Build. Mater.* 141, 526–532.
- Biligiri, K.P., Kaloush, K.E., Mamlouk, M.S., Witzczak, M.W. (2007). Rational modeling of tertiary flow for asphalt mixtures. *Transp. Res. Rec.* 2001, 63–72.
- Bonaquist, R., Christensen, D.W. (2005). Practical procedure for developing dynamic modulus master curves for pavement structural design. *Transp. Res. Rec.* 1929, 208-217.
- Farina, A., Zanetti, M.C., Santagata, E., Blengini, A. (2017). Life cycle assessment applied to bituminous mixtures containing recycled materials: crumb rubber and reclaimed asphalt pavement. *Resour. Conserv. Recycl.* 117, 204–212.
- Jamshidi, A., Hamzah, M.O., You, Z. (2013). Performance of warm mix asphalt containing Sasobit: state-of-the-art. *Constr. Build. Mater.* 38, 530–553.
- Mogawer, W., Austerman, A., Mohammad, L., Kutay, M.E. (2013). Evaluation of high RAP-WMA asphalt rubber mixtures. *Road Mater. Pavement* 14, 129–147.
- Pouranian, M. R., and Shishehbor, M. (2019). Sustainability assessment of green asphalt mixtures: a review. *Environment* 6, 73.
- Saberi, K. F., Fakhri, M., Azami, A. (2017). Evaluation of warm mix asphalt mixtures containing reclaimed asphalt pavement and crumb rubber. *J. Cleaner Prod.* 165, 1125–1132.
- Santagata, E., Dalmazzo, D., Lanotte, M., Zanetti, M.C., Ruffino, B. (2012). Relationship between crumb rubber morphology and asphalt rubber viscosity. *Proceedings, 5th Asphalt Rubber International Conference*, 513-532.
- Santagata, E., Baglieri, O., Alam, M., Lanotte, M., Riviera, P.P. (2015). Evaluation of rutting resistance of rubberized gap-graded asphalt mixtures. *Proceedings, 6th International Conference Bituminous Mixtures and Pavements*, 407-412.
- Santagata, E., Lanotte, M., Baglieri, O., Dalmazzo, D., Zanetti, M.C. (2016). Analysis of bitumen-crum rubber affinity for the formulation of rubberized dry mixtures. *Mater. Struct.* 49, 1947-1954.
- Underwood, B.S., Baek, C., Kim, Y.R. (2012). Simplified viscoelastic continuum damage model as platform for asphalt concrete fatigue analysis. *Transp. Res. Rec.* 2296, 36–45.
- Xiao, F., Amirghanian, S., Juang, C. H. (2007). Rutting resistance of rubberized asphalt concrete pavements containing reclaimed asphalt pavement mixes. *J. Mater. Civ. Eng.* 19, 475-483.
- Xiao, F., Amirghanian, S., (2008) Resilient modulus behavior of rubberized asphalt concrete mixtures containing reclaimed asphalt pavement. *Road Mater. Pavement* 9, 633-649.
- Zanetti, M.C., Fiore, S., Ruffino, R., Santagata, E., Lanotte, M. (2014). Assessment of gaseous emissions produced on site by bituminous mixtures containing crumb rubber. *Constr. Build. Mater.* 67, 291-296.
- Zanetti, M.C., Fiore, S., Ruffino, R., Santagata, E., Dalmazzo, D., Lanotte, M. (2015). Characterization of crumb rubber from end-of-life tyres for paving applications. *Waste Manage.* 45, 161-170.